



Deposited via The University of Sheffield.

White Rose Research Online URL for this paper:

<https://eprints.whiterose.ac.uk/id/eprint/210427/>

Version: Published Version

---

**Article:**

Obande, W., Stankovic, D., Bajpai, A. et al. (2023) Thermal reshaping as a route for reuse of end-of-life glass fibre-reinforced acrylic composites. *Composites Part B: Engineering*, 257. 110662. ISSN: 1359-8368

<https://doi.org/10.1016/j.compositesb.2023.110662>

---

**Reuse**

This article is distributed under the terms of the Creative Commons Attribution (CC BY) licence. This licence allows you to distribute, remix, tweak, and build upon the work, even commercially, as long as you credit the authors for the original work. More information and the full terms of the licence here:

<https://creativecommons.org/licenses/>

**Takedown**

If you consider content in White Rose Research Online to be in breach of UK law, please notify us by emailing [eprints@whiterose.ac.uk](mailto:eprints@whiterose.ac.uk) including the URL of the record and the reason for the withdrawal request.



# Thermal reshaping as a route for reuse of end-of-life glass fibre-reinforced acrylic composites

Winifred Obande<sup>a</sup>, Danijela Stankovic<sup>a</sup>, Ankur Bajpai<sup>a</sup>, Machar Devine<sup>a</sup>, Christian Wurzer<sup>b</sup>, Anna Lykkeberg<sup>c</sup>, Jennifer A. Garden<sup>c</sup>, Conchúr M. Ó Brádaigh<sup>a</sup>, Dipa Ray<sup>a,\*</sup>

<sup>a</sup> School of Engineering, Institute for Materials and Processes, The University of Edinburgh, Sanderson Building, Robert Stevenson Road, Edinburgh, EH9 3FB, Scotland, United Kingdom

<sup>b</sup> School of GeoSciences, UK Biochar Research Centre, The University of Edinburgh, Edinburgh, EH9 3FF, Scotland, United Kingdom

<sup>c</sup> EaStCHEM School of Chemistry, The University of Edinburgh, Joseph Black Building, David Brewster Road, Edinburgh, EH9 3FJ, Scotland, United Kingdom

## ARTICLE INFO

Handling Editor: Uday Vaidya

## ABSTRACT

Thermal reshaping has been employed to simulate the end-of-life reuse of liquid-resin-infused thermoplastic acrylic composite laminates, and the associated effects on matrix-dominated mechanical performance and microstructure have been studied. *L-shaped* laminates were infused at room temperature and subjected to 1 or 4 hot-press flattening cycles (25 min at 120 °C; 11 bar). Compared to the original references, up to 13% higher transverse flexural strengths were measured for the reprocessed laminates. Such a scheme may be readily implemented for high-value reuse without sacrificing fibre length scales, and with minimal cumulative mass loss over successive reheating cycles (10 cycles: 2% and 15 cycles: 2.6%). This study provides important insights to foster a greater understanding of the performance limits of hot-press reprocessing to inform the practical reuse and re-application of sustainable composites in a circular economy.

## 1. Introduction

Fibre-reinforced polymer (FRP) composites continue to be attractive subjects for research, production and use across many sectors, owing to their exceptional specific strength and stiffness properties, and excellent application-specific tailorability for diverse environments and loading conditions (e.g.: corrosion and fatigue). From a reprocessibility point of view, thermoplastic (TP) matrices are superior to their thermosetting (TS) counterparts because their long polymer chains are not cross-linked, allowing for repeated melting and re-processing. However, high melt viscosities were historically a major limiting factor to the widespread use of thermoplastic fibre-reinforced polymers (TP-FRPs). More recently, advanced innovative reactive TP resin formulations have facilitated the fabrication of TP-FRPs using technologies that were once solely applicable to low-viscosity TS resins. In light of growing environmental concerns surrounding the depletion of fossil fuel resources, and the waste-related end-of-life legacy issues affecting several sectors, the timeliness of these advancements cannot be understated in enabling a shift from TS-FRPs, which are more challenging to reprocess [1]. Notwithstanding, sustainably meeting the demands posed by continued

composites market growth will require rigorous counterbalancing measures such as minimising the dependence on finite resources while improving resource efficiency [2,3]. As it stands, a projected 25 billion metric tonnes of plastic waste will be generated by 2050 if such measures are not effectively established and developed [4].

Various recycling technologies have been demonstrated and the most applied methods broadly fall under three categories. (i) Mechanical recycling involves the grinding or shredding of fibre-reinforced polymer composites into smaller fragments or pieces to be reused by moulding. (ii) Pyrolysis involves the conversion of waste composite materials into gaseous volatiles, char, and recovered fibres by heating under inert atmospheres between 350 °C and 800 °C (iii) Finally, solvolysis employs solvents (e.g.: supercritical fluids and catalytic solutions). as depolymerisation or bond-breaking media for fibre and matrix recovery [4–11]. Although mechanical recycling is widely applied due to the requirement for relatively low energy and the absence of harsh solvents, the reduction in fibre length scales can result in considerable losses of performance. Moreover, compared to pyrolysis, solvolysis can offer the advantage of requiring lower temperatures and producing clean, char-free fibre surfaces; however, the negative environmental and

\* Corresponding author.

E-mail address: [dipa.roy@ed.ac.uk](mailto:dipa.roy@ed.ac.uk) (D. Ray).

<https://doi.org/10.1016/j.compositesb.2023.110662>

Received 28 December 2022; Received in revised form 19 February 2023; Accepted 4 March 2023

Available online 6 March 2023

1359-8368/© 2023 The Authors. Published by Elsevier Ltd. This is an open access article under the CC BY license (<http://creativecommons.org/licenses/by/4.0/>).

health impacts of solvents and catalysts may often outweigh the benefits [12].

As thermoplastic monomeric and oligomeric resins such as the Elium® family of acrylic resins by Arkema continue to grow in popularity, more and more research efforts have been invested in establishing a comprehensive database of performance and applicability [13–20]. While some recent works have been published addressing the gaps in end-of-life recycling and reuse [21–24], the effects of thermal reshaping on performance remain substantially unexplored except for previous research by Cousins et al. [24] where the reuse potential of large-scale acrylic-matrix composites was demonstrated by thermoforming among other techniques. Current waste management strategies are insufficiently developed, placing undue emphasis on the lower tiers of the waste hierarchy instead of prioritising value maximization. This will undoubtedly need to be addressed to offset current and future landfilling rates.

Reusing and repurposing end-of-life materials, e.g.: from decommissioned large-scale wind turbine blades provide attractive pathways for energy and resource recovery in line with the waste management hierarchy. Moreover, reuse via thermal reshaping bypasses the challenges associated with traditional fibre and matrix separation processes, as well as those emanating from the collection, sorting and realignment of reclaimed fibres [25]. Nonetheless, there is a considerable lack of published literature exploring the effects of thermal reshaping on residual performance. Such studies are essential in building a comprehensive performance database for improved reliability and confidence and may drive the rapid adoption of high-value reused composites into the future.

Thus, this study aims to simulate and evaluate an end-of-life, hot-press-based reshaping and reprocessing scheme for applicability to glass fibre-reinforced acrylic composites to maximise the benefit of higher fibre length scales and enhance performance. To offer additional insights, thermogravimetric analysis (TGA), dynamic mechanical analysis, and solution-state nuclear magnetic resonance and size exclusion chromatography using gel permeation chromatography have been employed. Static and cyclic isothermal TGA has also been used to simulate prolonged and repeated thermal cycling, respectively.

## 2. Materials and methods

### 2.1. Materials

This work employed a liquid thermoplastic acrylic resin (Elium® 180 – Arkema GRL, France), *in situ* polymerised with a dibenzoyl peroxide

initiator (BP-50-FT) supplied by United Initiators GmbH, Germany. Laminates comprised 4 plies ( $[90]_4$ ) of a glass fibre non-crimp fabric (TEST2594) supplied by Ahlstrom-Munksjö Glassfibre OY, Finland. The quasi-unidirectional fabric construction included glass fibres in the  $0^\circ$ - ( $600 \text{ g/m}^2$ ) and  $90^\circ$ - ( $36 \text{ g/m}^2$ ) directions, as well as PES stitching ( $10 \text{ g/m}^2$ ).

### 2.2. Laminate fabrication and thermal reshaping

#### 2.2.1. Liquid resin infusion

*L-shaped* laminates were produced by liquid resin infusion at room temperature using a custom steel mould. 4 plies of glass NCF were used for a target thickness of 2 mm, with the  $0^\circ$  fibre axes coinciding with the seam line as indicated by the superimposed arrows on all laminates in Fig. 1 (Steps 2–6). Following resin infusion, laminates were left to polymerise at room temperature for 24 h before demoulding.

**2.2.1.1. Platen press reprocessing and reshaping.** Once demoulded, *L-shaped* laminates were trimmed as illustrated in Fig. 1 (Step 2) to obtain a vertical height of 134 mm and target flattened dimensions of  $380 \text{ mm}$  [ $90^\circ$ ]  $\times$   $280 \text{ mm}$  [ $0^\circ$ ] as shown in Fig. 1 – Step 3. Original reference samples were extracted from the offcuts of the *as-infused* laminate (Fig. 1 – Step 2). These samples will hereafter be referred to as  $R \times 0$  samples. Similarly, samples extracted after reprocessing once and four times are denoted  $R \times 1$  and  $R \times 4$ , respectively.

Flattening was carried out by subjecting the laminates to a thermal cycle on a Pinette Emidecau Industries Heated Platen Press (Model: Lab 450 P) on preheated platens ( $120^\circ \text{C}$ ). For Step 3 (Fig. 1), a stepwise platen closure approach was adopted to produce the flattened components, with incremental closure every 5 min until the laminate had been flattened, as depicted in Fig. 2. This was done to facilitate progressive chain relaxation within the thermoplastic polymer matrix and to prevent damaging the component under rapid loading. Finally, at full platen closure, the components were held at  $120^\circ \text{C}$  for a further 5 min at 11 bar consolidation pressure. The components were actively cooled ( $10^\circ \text{C}/\text{min}$ ) to  $40^\circ \text{C}$  while maintaining pressure and were removed thereafter. Graphical overviews of the processing cycles are shown in Fig. 2.

The fibre and void volume fractions for the  $R \times 0$ ,  $R \times 1$  and  $R \times 4$  laminates were determined by the burn-off technique (ASTM D3171) and are summarised in Table 1 with corresponding thicknesses. Samples were extracted using a water-lubricated, diamond-coated saw blade and dried in a convection oven at  $50^\circ \text{C}$  overnight to remove residual moisture from the cutting process. Further details of test specimen

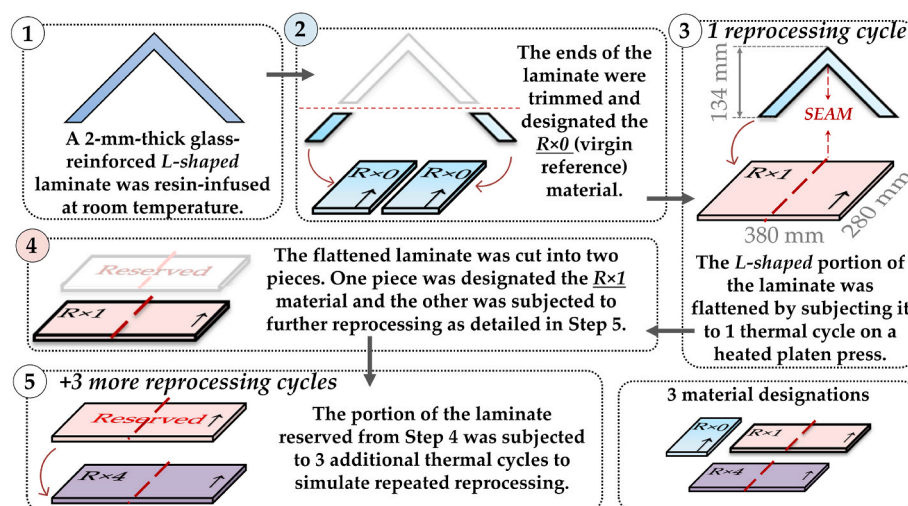


Fig. 1. Graphical representation of the *L-shaped* laminate production and reprocessing sequence. The overlaid arrows on each laminate indicate the corresponding fibre directions.

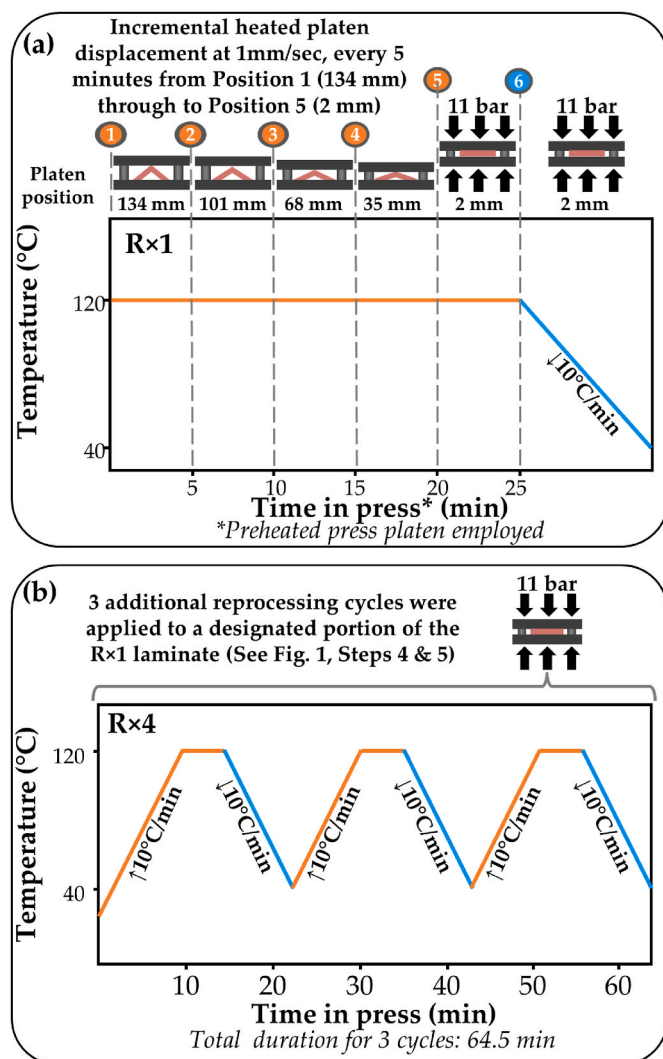


Fig. 2. A graphical representation of the reprocessing cycle parameters employed for (a)  $R \times 1$  and (b)  $R \times 4$  laminates. Details of platen positions, temperatures and applied pressures are provided where applicable.

Table 1

Summary of fibre and void volume fractions for virgin ( $R \times 0$ ), and reprocessed ( $R \times 1$  and  $R \times 4$ ) glass fibre-reinforced acrylic samples determined using the resin burn-off method. Results were averaged from triplicates.

	$R \times 0$	$R \times 1$	$R \times 4$
Fibre volume fraction (%)	$47.4 \pm 0.7$	$47.9 \pm 0.8$	$48.6 \pm 0.4$
Void volume fraction (%)	$2.0 \pm 0.3$	$2.0 \pm 1.0$	$2.0 \pm 0.3$
Laminate thickness (mm)	$2.15 \pm 0.04$	$2.10 \pm 0.04$	$2.10 \pm 0.06$

preparation and characterisation techniques are provided in the corresponding sections.

### 2.3. Transverse flexural testing

Samples measuring  $154 \text{ mm} \times 13 \text{ mm}$  were extracted for the determination of transverse flexural properties (strengths and moduli) by three-point bending in accordance with ASTM D7264. A span-to-thickness ratio of 32:1, corresponding to sample lengths of 154 mm and a crosshead speed of 1 mm/min were employed. Loading nose and supports used were hardened steel pins of 6 mm diameter. Testing was performed on an Instron (3369) test frame fitted with a 10 kN load cell (Instron 2530-10 kN) while mid-span deflections were tracked and

recorded via non-contact video extensometry. An illustration of the extraction scheme for flexural test specimens is presented in Fig. 3.

### 2.4. Dynamic mechanical analysis (DMA)

Longitudinal test samples with nominal measurements,  $60 \text{ mm} \times 10 \text{ mm}$  were extracted from seam-free regions and subjected to DMA testing in accordance with BS ISO 6721-11 for the determination of thermo-mechanical properties. Note that samples were extracted from the seam-free regions of each laminate, with the longitudinal axes coinciding with the fibre direction indicated by the arrow in Fig. 3. A TA Instruments Discovery DMA 850 was used in three-point bending mode. Samples were heated from ambient temperature to  $180 \text{ }^\circ\text{C}$  at  $3 \text{ }^\circ\text{C}/\text{min}$  and dynamically loaded at a frequency of 1 Hz and an amplitude of  $10 \text{ }\mu\text{m}$ . Storage and loss moduli and tan delta were recorded as functions of temperature throughout testing. Three samples were tested for each condition ( $R \times 0$ ,  $R \times 1$  and  $R \times 4$ ), for a total of 9 samples.

### 2.5. Thermogravimetric analysis

A Mettler Toledo TGA/DSC 1 analyser was used in this work in three ways. Firstly, dynamic thermogravimetric analysis (TGA) was used to assess the thermal stability and decomposition behaviour of the  $R \times 0$ ,  $R \times 1$ , and  $R \times 4$  materials in air by heating from ambient temperature to  $800 \text{ }^\circ\text{C}$  at a rate of  $10 \text{ }^\circ\text{C}/\text{min}$ . Secondly, the TGA instrument was used to simulate 15 successive reprocessing cycles with isothermal holds at  $120 \text{ }^\circ\text{C}$  for 60 min to determine the cumulative mass loss at Cycle 15; the total duration at  $120 \text{ }^\circ\text{C}$  is 900 min. Thirdly, the effect of prolonged heating (900 min) at  $120 \text{ }^\circ\text{C}$  on the evolution of mass loss was studied. For each TGA study type, samples weighing approximately 15 mg were analysed in duplicates.

### 2.6. Solution-state nuclear magnetic resonance (NMR) spectroscopy and size exclusion chromatography (SEC)

The polymer matrices from virgin ( $R \times 0$ ) and reprocessed ( $R \times 1$  and  $R \times 4$ ) materials were analysed by NMR spectroscopy to investigate any change in the chemical structure due to degradation. Fibre-reinforced samples were immersed in chloroform to dissolve the matrix phase, and the glass fibres were removed by filtration. The solvent was subsequently evaporated to produce a transparent film of acrylic matrices. All samples were soluble in other common solvents, specifically acetone and tetrahydrofuran (THF). The chemical structures of the recovered matrix films for all conditions ( $R \times 0$ ,  $R \times 1$  and  $R \times 4$ ) were compared using  $^1\text{H}$  and 2D NMR experiments (Diffusion-Ordered Spectroscopy (DOSY)). NMR spectra were recorded on a Bruker AVA500 (USA) spectrometer (500 MHz) at 298 K in  $\text{CDCl}_3$  and referenced to the residual  $\text{CDCl}_3$  peak ( $^1\text{H}$ :  $\delta$  7.26 ppm).

For SEC analysis, the recovered polymer matrix was dissolved in Gel permeation chromatography (GPC)-grade THF and filtered using a  $0.2 \text{ }\mu\text{m}$  PTFE syringe filter. Each sample was run at a flow rate of  $1 \text{ mL min}^{-1}$  at  $35 \text{ }^\circ\text{C}$  on a 1260 Infinity II GPC/SEC single detection system with two mixed bed C PLgel columns ( $300 \text{ mm} \times 7.5 \text{ mm}$ ). Molecular weights were obtained based on a calibration curve of narrow molecular weight distribution polystyrene.

## 3. Results and discussion

### 3.1. Transverse flexural test results

Results obtained from *no seam* samples from  $R \times 1$  and  $R \times 4$  conditions (Fig. 5) will be directly compared to the virgin/*as infused*,  $R \times 0$  samples to quantify the residual performance after thermal processing and the effects of successive reprocessing operations. Unflipped *seam* samples (as defined in Fig. 3) will be directly compared with *no seam* samples within the same condition ( $R \times 1$  or  $R \times 4$ ) to gain insights into

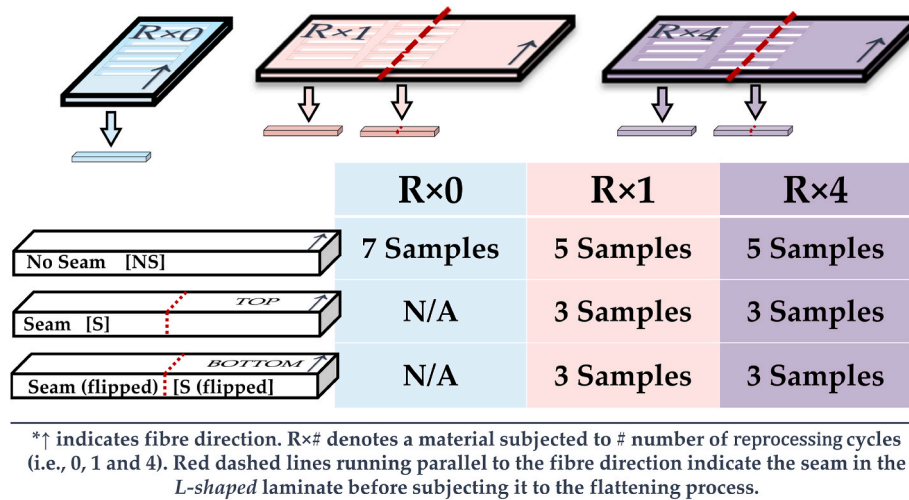
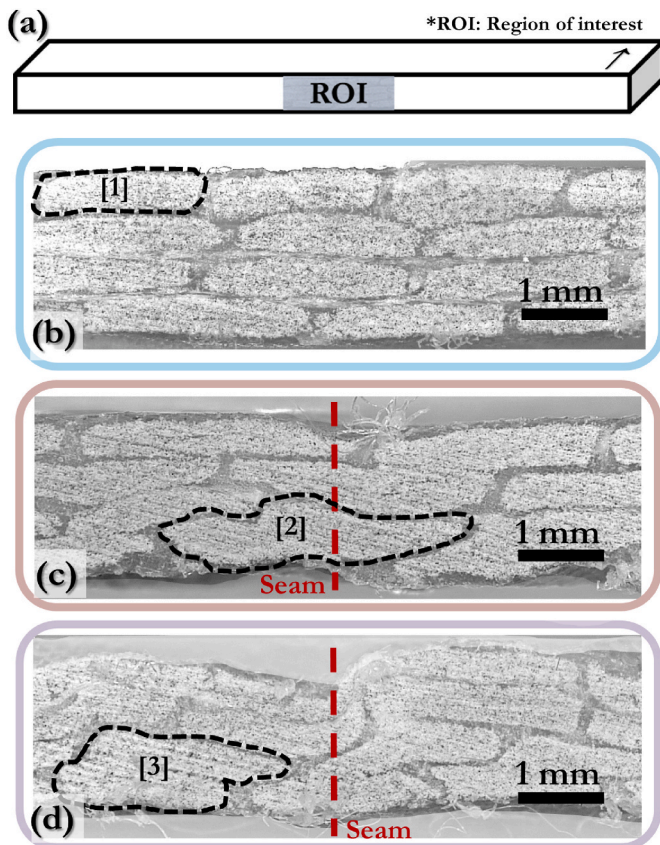


Fig. 3. A graphical representation of the transverse flexural test sample extraction scheme for all conditions [R × 0, R × 1 and R × 4] and all configurations [no seam and seam (flipped and unflipped)]. Test samples measured 154 mm × 13 mm × 2 mm. Superimposed black arrows depict the fibre direction in each laminate.



[1] Uniform tows; [2] & [3] Severe tow nesting and distortion. The Red dashed line indicates the seam line along the untested samples.

Fig. 4. (a) A graphical representation of the region of interest (ROI) designated for cross-sectional microscopic inspections on glass fibre-reinforced acrylic samples after (b) 0, (c) 1, and (d) 4 reprocessing cycles. Note: samples were cut in the direction transverse to the 0° fibres. Fibre volume fractions for these materials in order of increasing reprocessing cycles are 47.4%, 47.9% and 48.6%.

the effects of seam inclusion during thermal reshaping for the reuse of curved structures. Similarly, the comparisons between unflipped and flipped seam samples are intended to inform on the effects of primary

form/shape and hot-press reprocessing on structural integrity and function during the secondary (R × 1) and quinary (R × 4) reapplication of these materials.

3.1.1. The effects of the number of processing cycles on flexural properties

Fig. 5 shows the transverse flexural stress-strain curves for the virgin R × 0 samples (Fig. 5a), the reprocessed R × 1 (Fig. 5b) and R × 4 (Fig. 5c) samples. All samples exhibit similar linear elastic regions in terms of the evolution of stress with strain, with varying extents of minor load drops (from damage development) leading up to failure. R × 1\_NS-2, -4, and -5, however (Fig. 5b), had slightly higher strengths and failure strains (~3%). This may be due to more 0° tows remaining intact within these samples during damage evolution, resulting in the retention of load-bearing capacity between 1% and 3% strain. In addition, R × 1 samples, particularly R × 1\_NS-1 (Fig. 5b) exhibited a more distinct damage initiation point before the damage evolution region. The damage evolution behaviour of all samples suggests the occurrence and development of fragmentation and delamination processes, with more extensive damage occurring in R × 1\_NS samples.

It can also be observed that hot-press reprocessing results in an increase in both flexural strength and modulus as shown in Fig. 5d, where the R × 1 material exhibited 13% and 9% higher mean strength and modulus than those measured for its R × 0 counterpart (77.1 MPa and 7.2 GPa), respectively. However, when compared using an unpaired, one-tailed, two-sample Welch t-test with a significance level of 0.05 (refer to S1.3), it was found that only the strength value was statistically significant at p < 0.05.

Interestingly, a similar increase in flexural performance was reported for thermally aged (annealed) carbon fibre-reinforced acrylic composites by Bhudolia et al. [13], who ascribed this improvement to the positive effects of thermally-induced polymerisation of trapped monomeric residues within the composite laminates. However, the absence of discernible changes in matrix chemistry between R × 0, R × 1 and R × 4 as discussed in Section 3.4 suggests the influence of other factors. In general, transverse direction performance is dominated by matrix and fibre-matrix interfacial properties [26,27]; thus, taken together with the NMR and SEC results in Section 3.4, the changes in laminate thickness between R × 0 (2.15 ± 0.04 mm), R × 1 (2.1 ± 0.4 mm) and R × 4 (2.1 ± 0.6 mm) suggest that the reprocessing route employed herein may enhance fibre/matrix adhesion and enables more effective load transfer [28].

3.1.2. The effects of seam inclusion and orientation on flexural properties

Fig. 6 presents direct comparisons of the flexural properties of seam-

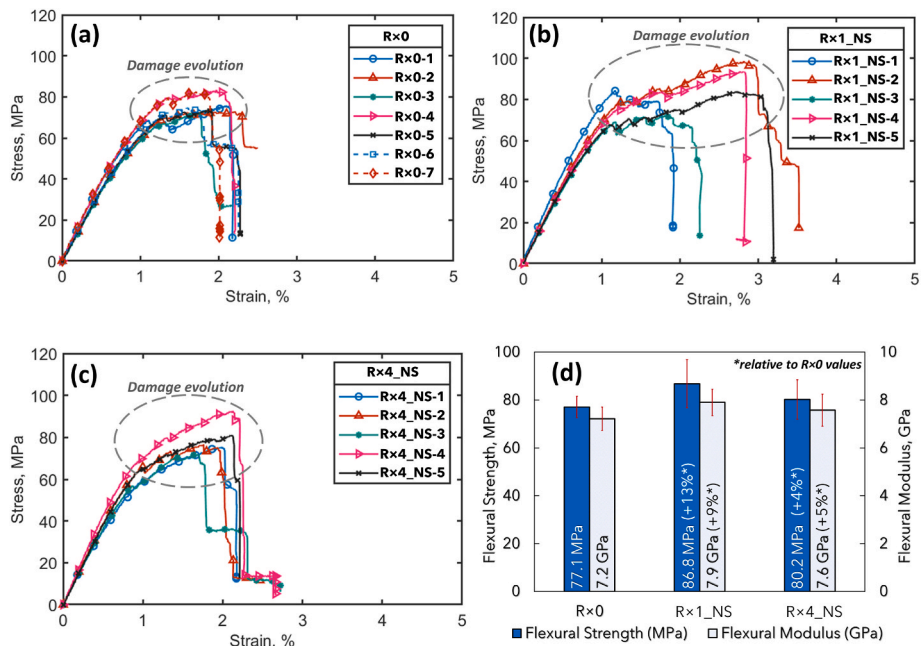


**Fig. 5.** Transverse flexural stress-strain curves showing the effects of reprocessing cycles on glass fibre-reinforced composites where the # “R × #” indicates the number of reprocessing cycles employed in (a) R × 0, (b) R × 1, and (c) R × 4; and (d) average transverse flexural strengths and moduli for these materials. Fibre volume fractions for these materials in order of increasing reprocessing cycles are 47.4%, 47.9% and 48.6%.

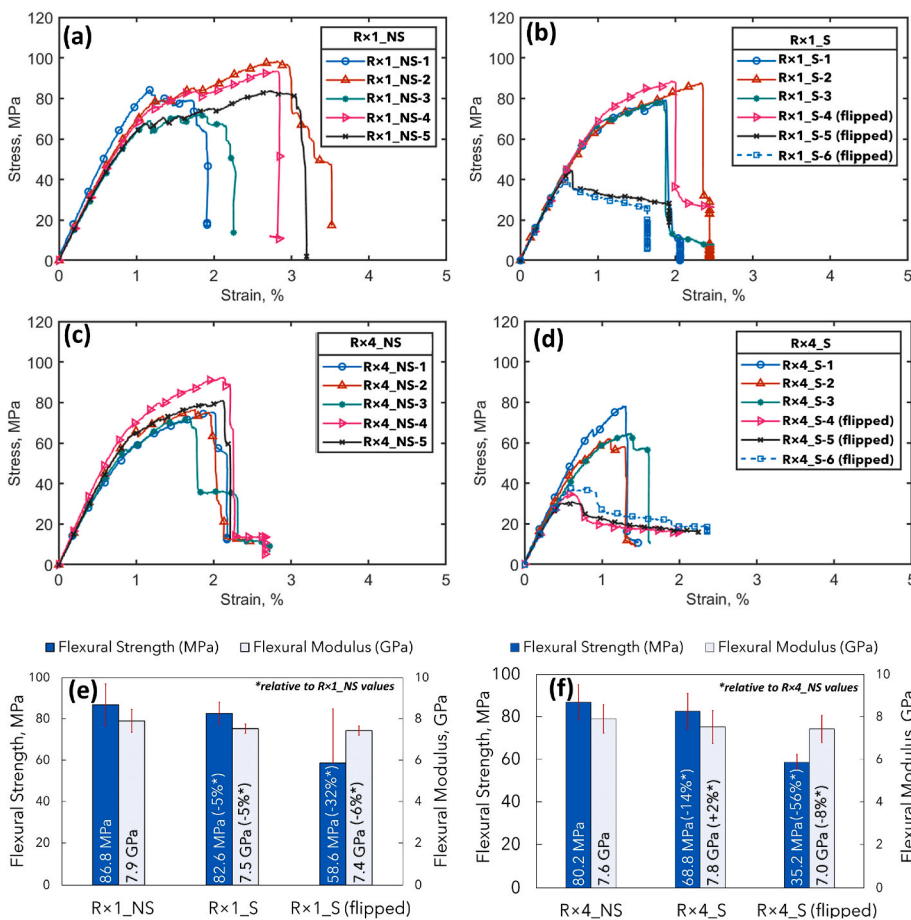


**Fig. 6.** Stress-strain curves showing the effects of thermal reshaping on (a), (c) seam-free and seam-containing (b), (d) glass fibre-reinforced composite materials. Bar charts showing the average transverse flexural strengths and moduli for (e) R × 1 and (f) R × 4 samples where × 1 and × 4 indicate the number of reprocessing cycles. NS and S indicate the absence and presence of seams in the samples, respectively. Fibre volume fractions for R × 1 and R × 4 are 47.9% and 48.6%, respectively.

containing samples with their seam-free counterparts. Depending on the presence and orientation of seams with respect to applied loads, reprocessed components can exhibit considerable reductions in strengths and moduli.

While all samples appear to exhibit the same linear stress-strain evolution Fig. 6 (a)-(c), unflipped *seam* samples ( $R \times 1_S$ -1,  $R \times 1_S$ -2, and  $R \times 1_S$ -3) and ( $R \times 4_S$ -1,  $R \times 4_S$ -2, and  $R \times 4_S$ -3): Fig. 6b and d) appear to fail at lower stresses and strains than their seam-free counterparts ( $R \times 1_{NS}$  samples).

The presence of a seam in  $R \times 1_S$  results in 5% reductions in both strength and modulus compared to its seam-free counterpart  $R \times 1_{NS}$ . Similarly,  $R \times 4_S$  samples exhibit 14% lower strength values compared to  $R \times 4_{NS}$  samples. These differences are statistically significant at  $p < 0.05$  as shown in S1.3. The reductions in strength are plausibly due to the pronounced structural non-uniformities, and tow distortions within the seam-containing samples as previously shown in Fig. 4. All average strengths and moduli are presented in Fig. 6e.

The most considerable losses in strength resulted from flipping the samples for testing as illustrated in Fig. 3. The  $R \times 1_S$  (flipped) and  $R \times 4_S$  (flipped) samples exhibited 32% and 56% lower transverse flexural strengths than the  $R \times 1_{NS}$  and  $R \times 4_{NS}$ , respectively. While these differences were statistically significant, only negligible losses (6% and 8%) were observed for corresponding modulus values. Overall,  $R \times 1_S$  (flipped) and  $R \times 4_S$  (flipped) samples (Fig. 6b, Fig 6d and 6e) had shorter linear stress-strain evolutions, with earlier onset of failure than all other samples, characterised by massive load drops followed by high-strain material failure events. The load drop event suggests the occurrence of  $0^\circ$  tow rupture and/or delamination propagation within these samples. These findings suggest that strategic redesign for reuse must not only account for the presence of seams resulting from complex geometries but must factor in the orientations employed during reforming operations and subsequent re-application. Such considerations will even be more crucial for constructions using longitudinal reinforcements, where kinking and geometrical distortions can have catastrophic effects.

To provide insights for interpreting the results of mechanical testing, microscopic inspections were conducted on the cross-section of seam-containing  $R \times 1$  and  $R \times 4$  samples alongside an  $R \times 0$  sample. Samples were cut in the direction transverse to the  $0^\circ$  fibres, with the cross-sectional region of interest along the cut plane as shown in Fig. 4a. The micrographs revealed distinct characteristics in the reprocessed materials  $R \times 1$  (Fig. 4c) and  $R \times 4$  (Fig. 4d) from those in the virgin reference  $R \times 0$  (Fig. 4b).

Given that these micrographs were obtained from untested samples from each material, the observed surface undulations, tow nesting and distortions in  $R \times 1$  (Fig. 4c) and  $R \times 4$  (Fig. 4d) are associated with the thermal reshaping process. While the  $R \times 0$  material appears to have similar sizes of ellipsoidal tows stacked uniformly with minor resin-rich gaps, the irregularities produced by tow form distortion and nesting result in the formation of some highly packed fibre zones interspersed with resin-rich zones.

### 3.2. Dynamic mechanical analysis

Dynamic mechanical analysis (DMA) has been used to assess any microstructural changes within the polymer matrix to complement the investigations discussed in Section 3.4. For instance, any increase in crosslink density within crosslinked polymers can be revealed by an increase in the glass transition temperature ( $T_g$ ) and a decrease in the loss factor ( $\tan \delta$ ) [29,30]. The DMA thermograms obtained for this work are presented in Fig. 7a-Fig. 7c.

Apart from slight changes to the apparent repeatability across the triplicates within the three sets of materials, no significant changes in  $T_g$  were observed as a result of reprocessing, with values of  $124^\circ\text{C}$ – $125^\circ\text{C}$  measured for all materials. As shown in Fig. 7d, only marginal increases of 0.8% and 0.7% were measured in  $T_g$  for the  $R \times 1$  and  $R \times 4$  materials relative to the virgin reference ( $R \times 0$ ), respectively. The corresponding increases in the  $\tan \delta$  peak of 1.8% and 12.5% suggest the unlikelihood of cross-link formation as a result of thermo-oxidative degradation of the matrix during the hot-press reprocessing steps.

### 3.3. Thermogravimetric analysis

#### 3.3.1. Dynamic thermogravimetric analysis to evaluate stability

Taken together with the graphical legend in Fig. 8, Table 2 presents an overview of the results shown in Fig. S1 from thermogravimetric analysis of glass fibre-reinforced acrylic materials. Although the samples differ by the number of reprocessing cycles (0, 1, and 4), all samples underwent a similar degradation process to that of the unreinforced acrylic matrix of identical composition (under a nitrogen atmosphere) as reported in the authors' previous work [17]. The interested reader may refer to the TGA results for "A100/P0" in the cited study.

From the results presented in Table 2, it can be seen that while no discernible trends were observed for the temperatures corresponding to mass losses of 5% and 10% for all sets, clear trends can be seen in the

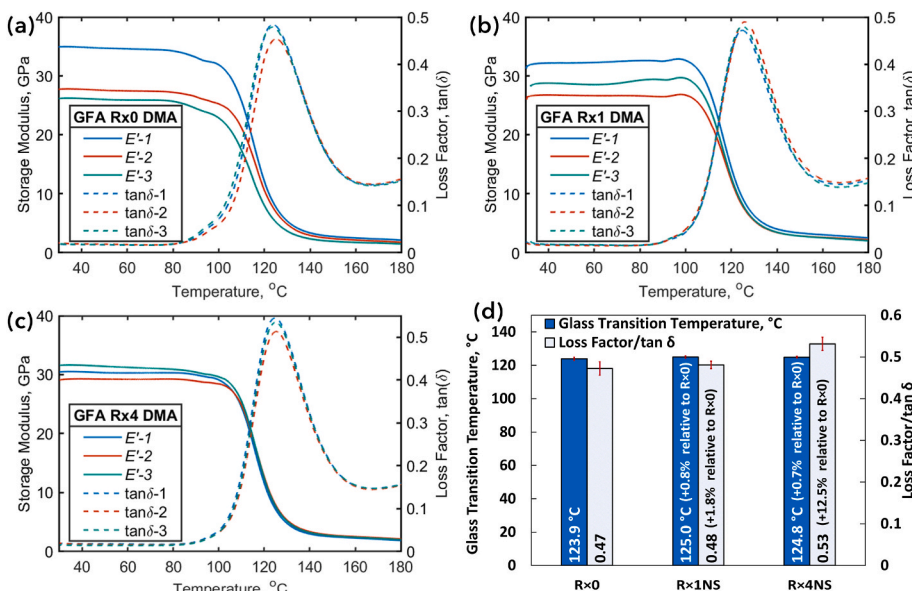
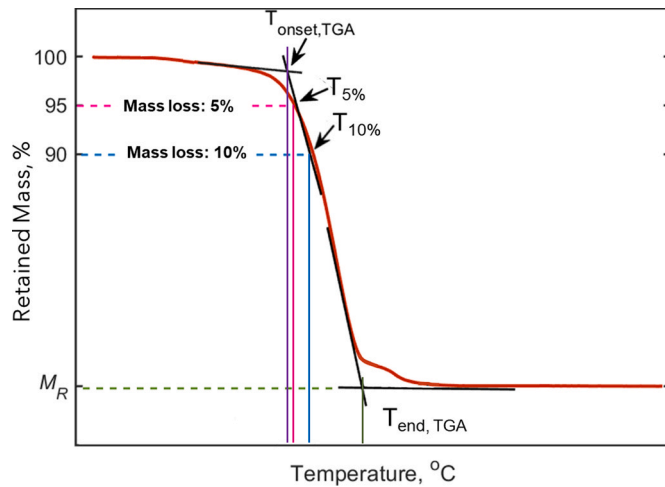


Fig. 7. Dynamic mechanical analysis thermograms showing the evolution of storage moduli ( $E'$ ) and loss factor ( $\tan \delta$ ) with temperature for (a) virgin  $R \times 0$ , and the hot-press reprocessed (b)  $R \times 1$  and (c)  $R \times 4$  glass fibre-reinforced acrylic materials; and (d) a bar chart showing the average glass transition temperatures and loss factor/ $\tan \delta$  as functions of the number of reprocessing cycles (0, 1 and 4). Fibre volume fractions for these materials in order of increasing reprocessing cycles are 47.4%, 47.9% and 48.6%.



**Fig. 8.** Idealised scheme of a TGA thermogram, showing the parameters of interest reported within this work as presented in Table 2. Note,  $M_R$  indicates the residual mass fraction, whereas  $T_{5\%}$  and  $T_{10\%}$  indicate the temperatures associated with the 5 % and 10% mass losses.

**Table 2**

Thermogravimetric analysis results for glass fibre-reinforced acrylic composites subjected to 0, 1 and 4 hot-press reprocessing cycles. Refer to Fig. 8 for a graphical legend of the presented data.

	$T_{onset,TGA}$	$T_{5\%}$	$T_{10\%}$	$T_{end,TGA,1}$	$M_R(\%)$
$R \times 0$	$285 \pm 0$	$279 \pm 0.5$	$301 \pm 1.2$	$376 \pm 0$	$56 \pm 0.1$
$R \times 1$	$280 \pm 0.1$	$276 \pm 1.4$	$297 \pm 1.3$	$381 \pm 0.9$	$56 \pm 0.4$
$R \times 4$	$270 \pm 3$	$278 \pm 5$	$301 \pm 3.8$	$392 \pm 4.7$	$65 \pm 1.5$

Note, that the fibre mass fractions (determined using the burn-off method) for the  $R \times 0$ ,  $R \times 1$ , and  $R \times 4$  laminates were  $67 \pm 0.6\%$ ,  $67.4 \pm 0.4$ , and  $68.1 \pm 0.3$ , respectively. Any deviation of the residual masses ( $M_R$ ) from these values may be attributed to minor differences in the samples owing to the small sample quantities (approx. 15 mg) required for TGA investigations. Thus, these results suggest that all three materials are virtually identical from a thermal stability point of view and that reprocessing does not appear to have any deleterious effects in this regard.

onset and endset temperatures, and residual masses.

Where trends exist, only marginal changes occur for all parameters. Increasing the number of reprocessing cycles appears to decrease the onset temperature by 5% from  $285 \text{ }^\circ\text{C}$  ( $R \times 0$ ) to  $270 \text{ }^\circ\text{C}$  ( $R \times 4$ ). Conversely, the endset temperature increases by up to 4% and the residual mass increases from 56% to 65%.

### 3.3.2. Isothermal thermogravimetric simulations of extended reprocessing

TGA-based simulations of extended thermal reprocessing were performed to explore the limits of reprocessing with glass fibre-reinforced acrylic composites. The results of cyclic and prolonged isothermal experiments are presented in Fig. 9.

Beginning with the cyclic simulation, the corresponding mass losses for processing these materials in air can be predicted. After 1 processing cycle at  $120 \text{ }^\circ\text{C}$  for 1 h, a mass loss of 1.5% can be expected; similarly, the 4-cycle and 15-cycle losses are predicted to be 2% and 2.6%, respectively. There appears to be a distinct transition stage of mass loss associated with the cyclic processing scheme (Fig. 9a), characterised by a plateau at about 2% mass loss between Cycles 4 and 10. This stage precedes the final stage for this duration, where a further 0.6% of mass loss occurred. Interestingly, the cumulative mass loss predicted is slightly higher than that resulting from prolonged isothermal heating at  $120 \text{ }^\circ\text{C}$  for the same duration as the isothermal phases of the cyclic experiment (Fig. 9a); only 2.05% is predicted to occur.

It is likely that beyond 10 cycles, some microstructural changes begin

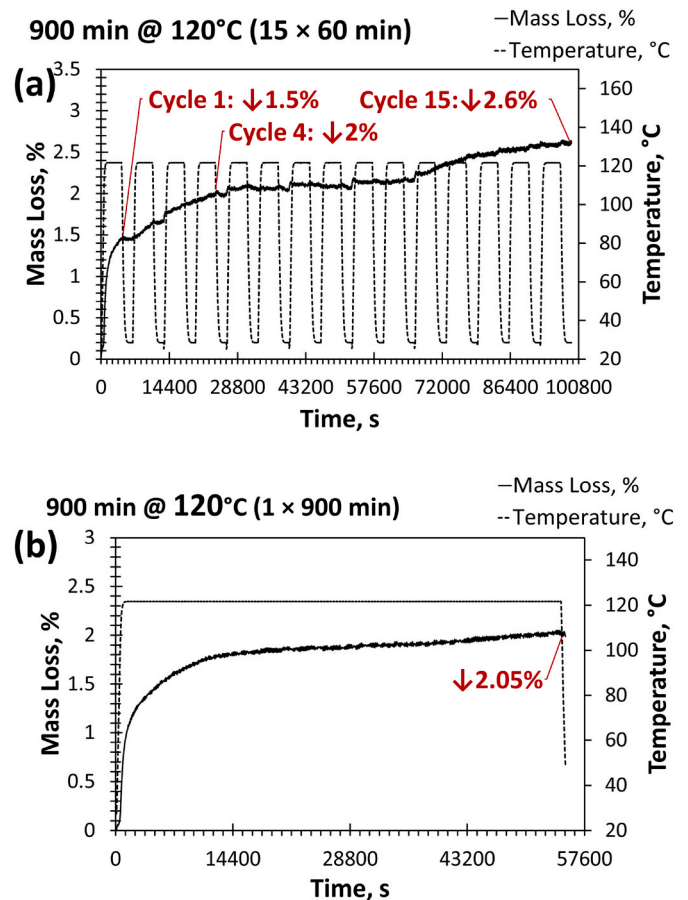


**Fig. 9.** Results of isothermal thermogravimetry simulations of (a) successive cycles and (b) a single prolonged thermal reprocessing cycle.

to occur due to thermal degradation. It is worth mentioning, however, that the magnitudes of mass loss reported here are still relatively low.

### 3.4. Solution-state nuclear magnetic resonance (NMR) spectroscopy and size exclusion chromatography (SEC)

To evaluate if the thermal reshaping affected the chemical structure of the acrylic matrix of the samples, they were analysed by solution-state NMR spectroscopy in  $\text{CDCl}_3$  and SEC in THF. The acrylic matrix was removed from the glass fibres by dissolution in chloroform. The solvent was subsequently evaporated and the recovered polymer was dissolved in  $\text{CDCl}_3$  (NMR) and THF (SEC) respectively, prior to analysis. No significant solubility differences were observed between the samples when dissolving the polymer from the fibres, and all were soluble in chloroform, acetone and THF at room temperature. Cross-linked polymers typically demonstrate lower solubility than their non-cross-linked counterparts, and thus the comparable solubilities suggest that no cross-linking occurred under the thermal reshaping conditions. It is important to note that here, both SEC and NMR are used as solution-state analyses, thus only investigate the soluble components of the samples. However, visual examination showed freely floating glass fibres, indicating that no major polymeric fractions remained undissolved. Overall, these analyses provide complementary solution-state analysis of the matrix, the results of which align with the thermal and thermomechanical characterisation of the solid samples.

NMR spectroscopy is a technique that gives information on the different chemical functional groups present within the polymer structure. The solution-state  $^1\text{H}$  NMR spectra of the virgin and reprocessed samples were consistent with those observed for the acrylic matrix in previous work by the authors [17], there was evidence of the BPO

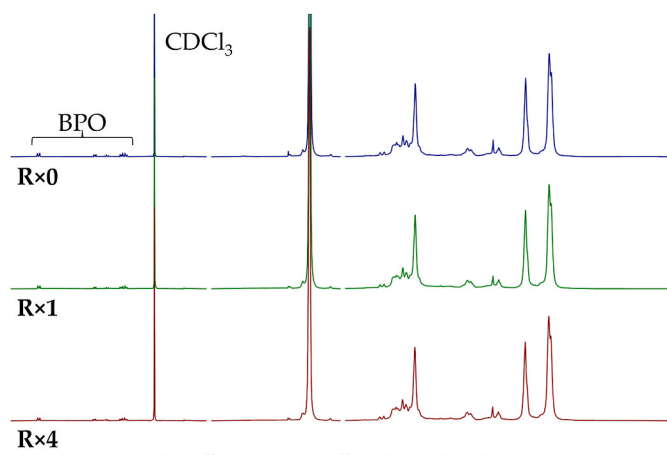


**Fig. 10.** Overlaid  $^1\text{H}$  NMR spectra of polyacrylic samples that were virgin ( $R \times 0$ ), or reprocessed once ( $R \times 1$ ) or four times ( $R \times 4$ ) in  $\text{CDCl}_3$ .

initiator (Fig. 10). No significant differences were observed between the  $^1\text{H}$  NMR spectra of the processed and unprocessed samples, which suggests that no significant structural changes have occurred. Traces of unknown species were also present, which may originate from impurities in starting materials and sample preparation, as well as small traces of the acrylic monomer (Fig. S2), potentially due to the polymerisation becoming diffusion limited at high conversions.

To further confirm the absence of structural change, the samples were also analysed by 2D DOSY NMR spectroscopy. DOSY NMR is a spectroscopic technique that separates components in a mixture according to their diffusion coefficient,  $D$ . The rate at which molecules diffuse through a solution is linked to their hydrodynamic radius, and thus enables insight into the relative molecular weights of polymers [31] due to the linear relationship between the logarithm of the diffusion coefficient ( $\log D$ ) and the molecular weight ( $\log M_w$ ). Introducing an average of even just one cross-link per polymer would double the molecular weight; this would lead to significant differences in diffusion times, which can be seen in DOSY NMR analysis. The spectra demonstrated that all three samples had comparable diffusion coefficients (Figs. S3–S5), supporting the conclusion that the acrylic matrix was not significantly affected by thermal reshaping. This was further probed by SEC analysis, as any potential cross-linking or degradation would impact molecular weights (increased or decreased respectively). The normalised SEC traces of all samples show a bimodal distribution (Fig. S6), common for radical polymerisations of acrylic monomers [32–34].

No significant differences were observed in the molecular weights upon thermal reshaping (Table 3). Detailed analysis revealed greater variation within the same sample than was observed between the virgin and reprocessed samples (Fig. S3 and Tables S2–S4). It should be noted that SEC separates polymers based on their hydrodynamic volume rather than absolute molecular weight. It could therefore be conceivable

**Table 3**

SEC results for virgin acrylic matrix sample  $R \times 0$  compared against thermally reprocessed samples  $R \times 1$  (reprocessed once) and  $R \times 4$  (reprocessed four times).

Sample <sup>a</sup>	$M_n \times 10^3$ ( $\text{g mol}^{-1}$ )	$M_w \times 10^3$ ( $\text{g mol}^{-1}$ )	$\mathcal{D}$
$R \times 0$ <sup>b</sup>	93.0	397.4	4.3
$R \times 1$ <sup>b</sup>	87.5	413.6	4.7
$R \times 4$ <sup>b</sup>	88.6	427.0	4.8

<sup>a</sup> Acrylic matrices isolated from fibres by dissolving in chloroform, filtering and drying. Samples were run in THF at  $35^\circ\text{C}$  at  $1\text{ mL min}^{-1}$  and calibrated against polystyrene standards.

<sup>b</sup> These results are all within experimental error of each other. See the Supplementary material, Fig. S6 and Tables S2–S4 for more detail.

that a cross-linked polymer could appear at comparable molecular weights to a non-cross-linked polymer due to the cross-links decreasing the hydrodynamic volume and therefore appearing smaller. The lack of differences in solubility, however, would support no cross-linking occurring. Taken together, the similar solubilities of the non-processed ( $R \times 0$ ) and thermally reprocessed ( $R \times 1$  and  $R \times 4$ ) samples, combined with the lack of significant differences observed in the solution-state  $^1\text{H}$  NMR spectroscopy, DOSY and SEC analysis suggests that no significant chemical changes have occurred in the acrylic matrix.

#### 4. Conclusions

In this study, the effects of hot-press reprocessing as a means of reusing end-of-life glass fibre-acrylic composites were examined using an L-shaped laminate ( $90^\circ$  bend). The laminate was flattened incrementally between platens heated at  $120^\circ\text{C}$  and re-processed thermally up to 4 times. Specimens were extracted from flat regions of the original and flattened/re-processed laminates. Additionally, the effects of including a seam from the flattened components with complex geometries were comprehensively assessed. To investigate the effects of the successive reprocessing cycles on the reclaimed material's properties, three conditions of reuse were studied: a virgin reference ( $R \times 0$ ), and two laminates subjected to 1 ( $R \times 1$ ) and 4 ( $R \times 4$ ) reprocessing cycles at  $120^\circ\text{C}$  under pressure (11 bar). Transverse flexural testing was performed along with TGA, and DMA. It was found that increasing the number of cycles results in higher transverse flexural strengths and moduli of up to 13% and 9% relative to the reference. No significant changes (<5%) were observed in the thermal stability of the reprocessed materials in the air. The glass transition temperature was maintained across the set at  $125^\circ\text{C}$ , whereas  $\tan \delta$  increased by up to 12.5%. The possible changes in the chemical structure of the re-processed acrylic matrix were investigated with solution-state NMR and SEC.  $^1\text{H}$  and DOSY NMR spectroscopy, and SEC analysis confirmed that no significant chemical change occurred under the three conditions employed in this work. Further insights were garnered from the results of simulated extended reuse studies via TGA. Cycling the glass fibre-reinforced acrylic material at  $120^\circ\text{C}$  for 60 min over 15 cycles revealed that 1-cycle and 4-cycle reprocessing can be expected to cause 1.5% and 2% mass losses, respectively. It was predicted that up to 10 cycles can be performed with negligible change in mass loss. From Cycles 10 to 15, however, a further 0.6% loss may be observed. These findings highlight unique opportunities for low-temperature, high-value reuse by thermally reshaping end-of-life continuous fibre-reinforced acrylic composites, providing insights into the associated effects on performance and limits of applicability – vital elements for realising environmental and economic benefits in the composites value chain.

#### CRedit author statement

**Winifred Obande:** Conceptualisation, methodology, investigation, project administration, formal analysis, writing – original draft preparation, writing – reviewing and editing

**Danijela Stankovic:** Project administration, investigation, formal analysis, visualisation, writing – reviewing and editing

**Ankur Bajpai:** Project administration, formal analysis, writing – reviewing and editing

**Machar Devine:** Project administration, writing – reviewing and editing

**Christian Wurzer:** Investigation, writing – reviewing and editing

**Anna Lykkeberg:** Investigation, formal analysis, writing – original draft preparation, writing – reviewing and editing

**Jennifer A. Garden:** Investigation, formal analysis, writing – original draft preparation, writing – reviewing and editing

**Conchúr M. Ó Brádaigh:** Supervision, writing – reviewing and editing.

**Dipa Ray:** Conceptualisation, supervision, resources, funding

acquisition, project administration, writing – reviewing and editing

### Declaration of competing interest

The authors declare that they have no known competing financial interests or personal relationships that could have appeared to influence the work reported in this paper.

### Data availability

Data will be made available on request.

### Acknowledgements

The authors wish to thank the Supergen ORE Hub for funding received through the Flexible Fund Award FF2021-1014. We would also like to acknowledge the following funding sources: EPSRC SOF12 Centre for Doctoral Training and Croda (A. L. EP/S023631/1); UKRI Future Leaders Fellowship (J. A. G. MR\T042710\1); and Royal Society (J. A. G. Grant RSG/R1/180101).

### Appendix A. Supplementary data

Supplementary data to this article can be found online at <https://doi.org/10.1016/j.compositesb.2023.110662>.

### References

- Obande W, Ó Brádaigh CM, Ray D. Continuous fibre-reinforced thermoplastic acrylic-matrix composites prepared by liquid resin infusion – a review. *Compos B Eng* 2021. <https://doi.org/10.1016/j.compositesb.2021.108771>.
- Mativenga PT, Sultan AAM, Agwa-Ejon J, Mbohwa C. Composites in a circular economy: a study of United Kingdom and South Africa. *Procedia CIRP* 2017;61. <https://doi.org/10.1016/j.procir.2016.11.270>.
- Joustra J, Flipsen B, Balkenende R. Circular design of composite products: a framework based on insights from literature and industry. *Sustain Times* 2021;13. <https://doi.org/10.3390/su13137223>.
- Khalid MY, Arif ZU, Ahmed W, Arshad H. Recent trends in recycling and reusing techniques of different plastic polymers and their composite materials. *Sustain Mater Technol* 2022;31. <https://doi.org/10.1016/j.susmat.2021.e00382>.
- Evens T, Bex GJ, Yigit M, De Keyzer J, Desplentere F, Van Bael A. The influence of mechanical recycling on properties in injection molding of fiber-reinforced polypropylene. *Int Polym Process* 2019;34. <https://doi.org/10.3139/217.3770>.
- Rani M, Choudhary P, Krishnan V, Zafar S. A review on recycling and reuse methods for carbon fiber/glass fiber composites waste from wind turbine blades. *Compos B Eng* 2021;215. <https://doi.org/10.1016/j.compositesb.2021.108768>.
- Meng F, Cui Y, Pickering S, McKechnie J. From aviation to aviation: environmental and financial viability of closed-loop recycling of carbon fibre composite. *Compos B Eng* 2020;200. <https://doi.org/10.1016/j.compositesb.2020.108362>.
- Liu W, Huang H, Zhu L, Liu Z. Integrating carbon fiber reclamation and additive manufacturing for recycling CFRP waste. *Compos B Eng* 2021;215. <https://doi.org/10.1016/j.compositesb.2021.108808>.
- Fernández A, Santangelo-Muro M, Fernández-Blázquez JP, Lopes CS, Molina-Aldareguia JM. Processing and properties of long recycled-carbon-fibre reinforced polypropylene. *Compos B Eng* 2021;211. <https://doi.org/10.1016/j.compositesb.2021.108653>.
- Utekar S VKS, More N, Rao A. Comprehensive study of recycling of thermosetting polymer composites – driving force, challenges and methods. *Compos B Eng* 2021; 207. <https://doi.org/10.1016/j.compositesb.2020.108596>.
- Pender K, Yang L. Regenerating performance of glass fibre recycled from wind turbine blade. *Compos B Eng* 2020;198. <https://doi.org/10.1016/j.compositesb.2020.108230>.
- Job S, Leeke G, Mativenga PT, Oliveux G, Pickering S, Shuaib NA. *Composites recycling : where are we now*. Compos UK 2016.
- Bhudolia SK, Joshi SC, Bert A, Di YB, Makam R, Gohel G. Flexural characteristics of novel carbon methylmethacrylate composites. *Compos Commun* 2019;13:129–33. <https://doi.org/10.1016/j.coco.2019.04.007>.
- Bhudolia SK, Gohel G, Fai LK, Barsotti RJ. Investigation on ultrasonic welding attributes of novel carbon/Elium®composites. *Materials* 2020;13:10–5. <https://doi.org/10.3390/ma13051117>.
- Obande W, Ray D, Ó Brádaigh CM. Viscoelastic and drop-weight impact properties of an acrylic-matrix composite and a conventional thermoset composite – a comparative study. *Mater Lett* 2019;238. <https://doi.org/10.1016/j.matlet.2018.11.137>.
- Kazemi ME, Shanmugam L, Chen S, Yang L, Yang J. Novel thermoplastic fiber metal laminates manufactured with an innovative acrylic resin at room temperature. *Compos Part A Appl Sci Manuf* 2020;138:106043. <https://doi.org/10.1016/j.compositesa.2020.106043>.
- Obande W, Gruszka W, Garden JA, Wurzer C, Ó Brádaigh CM, Ray D. Enhancing the solvent resistance and thermomechanical properties of thermoplastic acrylic polymers and composites via reactive hybridisation. *Mater Des* 2021;206:109804. <https://doi.org/10.1016/j.matdes.2021.109804>.
- Kazemi ME, Shanmugam L, Li Z, Ma R, Yang L, Yang J. Low-velocity impact behaviors of a fully thermoplastic composite laminate fabricated with an innovative acrylic resin. *Compos Struct* 2020;250:112604. <https://doi.org/10.1016/j.compstruct.2020.112604>.
- Pantelelis N, Bistekos E, Emmerich R, Gerard P, Zoller A, Gallardo RR. Compression RTM of reactive thermoplastic composites using microwaves and cure monitoring. *Procedia CIRP* 2020;85:246–51. <https://doi.org/10.1016/j.procir.2019.10.005>.
- de Andrade Raponi O, Barbosa LCM, de Souza BR, Ancelotti Junior AC. Study of the influence of initiator content in the polymerization reaction of a thermoplastic liquid resin for advanced composite manufacturing. *Adv Polym Technol* 2018;37: 3579–87. <https://doi.org/10.1002/adv.22142>.
- Gebhardt M, Chakraborty S, Manolakis I, Meiners D. Closed-loop room temperature recycling of Elium CFRPs and its influence on the 2nd generation composite properties. *J Sci Alliance Plast Technol* 2020;16:179–210.
- Gebhardt M, Manolakis I, Chatterjee A, Kalinka G, Deubener J, Pfnür H, et al. Reducing the raw material usage for room temperature infusible and polymerisable thermoplastic CFRPs through reuse of recycled waste matrix material. *Compos B Eng* 2021;216:108877. <https://doi.org/10.1016/j.compositesb.2021.108877>.
- Bel Haj Frej H, Léger R, Perrin D, Jenny P, Gérard P, Devaux JF. Recovery and reuse of carbon fibre and acrylic resin from thermoplastic composites used in marine application. *Resour Conserv Recycl* 2021;173. <https://doi.org/10.1016/j.resconrec.2021.105705>.
- Cousins DS, Suzuki Y, Murray RE, Samaniuk JR, Stebner AP. Recycling glass fiber thermoplastic composites from wind turbine blades. *J Clean Prod* 2019;209: 1252–63. <https://doi.org/10.1016/j.jclepro.2018.10.286>.
- Bennet L, Hailey J, Lomoro P, Fitzgeralds A, Fuller J, Lightfoot J. Sustainable decommissioning: wind turbine blade recycling. <https://doi.org/10.13140/RG.2.2.15202.86723>; 2020.
- De Kok JMM, Peijs T. Deformation, yield and fracture of unidirectional composites in transverse loading. 2. Influence of fibre-matrix adhesion. *Compos Part A Appl Sci Manuf* 1999;30. [https://doi.org/10.1016/S1359-835X\(98\)00171-7](https://doi.org/10.1016/S1359-835X(98)00171-7).
- Liu Z, Lei Y, Zhang X, Kang Z, Zhang J. Effect mechanism and simulation of voids on hydrothermal performances of composites. *Polymers* 2022;14. <https://doi.org/10.3390/polym14050901>.
- Tan W, Naya F, Yang L, Chang T, Falzon BG, Zhan L, et al. The role of interfacial properties on the intralaminar and interlaminar damage behaviour of unidirectional composite laminates: experimental characterization and multiscale modelling. *Compos B Eng* 2018. <https://doi.org/10.1016/j.compositesb.2017.11.043>.
- Bandzierz K, Reuvekamp L, Dryzek J, Dierkes W, Blume A, Bielinski D. Influence of network structure on glass transition temperature of elastomers. *Materials* 2016;9. <https://doi.org/10.3390/MA9070607>.
- Bao RY, Jiang WR, Liu ZY, Yang W, Xie BH, Yang MB. Balanced strength and ductility improvement of in situ crosslinked poly(lactide)/poly(ethylene terephthalate glycol) blends. *RSC Adv* 2015;5. <https://doi.org/10.1039/c5ra02575c>.
- Li W, Chung H, Daefler C, Johnson JA, Grubbs RH. Application of 1H DOSY for facile measurement of polymer molecular weights. *Macromolecules* 2012;45. <https://doi.org/10.1021/ma301666x>.
- Suzuki Y, Mishima R, Matsumoto A. Bulk polymerization kinetics of methyl methacrylate at broad temperature range investigated by differential scanning calorimetry. *Int J Chem Kinet* 2022. <https://doi.org/10.1002/kin.21564>.
- Charlier Q, Fontanier J-CC, Lortie F, Pascault J-PP, Gerard J-FF. Rheokinetic study of acrylic reactive mixtures dedicated to fast processing of fiber-reinforced thermoplastic composites. *J Appl Polym Sci* 2019;136:1–9. <https://doi.org/10.1002/app.47391>.
- O'Shaughnessy B, Yu J. Autoacceleration in free radical polymerization. 2. Molecular weight distributions. *Macromolecules* 1994;27. <https://doi.org/10.1021/ma00096a033>.